Chapter 8

A Computational Chemistry Approach for the Catalytic Cycle of AHAS

Eduardo J. Delgado

Additional information is available at the end of the chapter

http://dx.doi.org/10.5772/intechopen.73705

Abstract

Acetohydroxy acid synthase (AHAS) is a thiamin diphosphate (ThDP)-dependent enzyme involved in the biosynthesis of branched-chain amino acids (valine, leucine, and isoleucine) in plants, bacteria, and fungi. This makes AHAS an attractive target for herbicides and bactericides, which act by interrupting the catalytic cycle and preventing the synthesis of acetolactate and 2-keto-hydroxybutyrate intermediates, in the biosynthetic pathway toward the synthesis of branched amino acids, causing the death of the organism. Several articles on the catalytic cycle of AHAS have been published in the literature; however, there are certain aspects, which continue being controversial or unknown. This lack of information at the molecular level makes difficult the rational development of novel herbicides and bactericides, which act inhibiting this enzyme. In this chapter, we review the results from our group for the different stages of the catalytic cycle of AHAS, using both quantum chemical cluster and Quantum Mechanics/Molecular Mechanics approaches.

Keywords: AHAS, catalytic cycle, DFT, QM/MM

1. Introduction

Computational chemistry is a branch of chemistry in which quantum mechanics and/or molecular mechanics methods are implemented on computers for understanding and predicting the behavior of chemical systems from molecular information. It plays a key role in the rational design of drugs, biomolecules, organic and inorganic molecules, catalysts, and so on.

Amino acids are organic compounds containing amine ($–NH_2$) and carboxyl (–COOH) functional groups, along with a side chain (R group) specific to each amino acid. An essential amino acid is an amino acid that cannot be synthetized by the organism and consequently

must be supplied by the food. Unlike animals, plants and microorganisms have the biosynthetic machinery to synthesize all the essential metabolites required for their survival. These differences in the metabolic paths between plants and animals are the basis for the rational development of herbicides and bactericides, chemicals that interrupt the biosynthetic route to branched chain amino acids causing the death of the plant or bacteria. To achieve this goal, detailed knowledge of the mechanisms at the molecular level is essential.

Plants and bacteria utilize several enzymes for the biosynthesis of branched chain amino acids such as valine, leucine, and isoleucine, being acetohydroxy acid synthase (AHAS), the one which catalyzes the first common step, followed by the participation of other enzymes which finally lead to the formation of these essential amino acids [1–5].

AHAS requires for its catalytic role the cofactor thiamin diphosphate, ThDP, in addition to flavin-adenine dinucleotide (FAD) and a divalent metal ion, Mg^{2+}. FAD has no catalytic function, and Mg^{2+} is required to anchor the diphosphate moiety of ThDP in the active site. During catalysis by ThDP-dependent enzymes, the 4-mino-pyrimidine moiety can interconvert among four ionization/tautomeric states: the 4′-aminopyrimidine (AP), the N1′-protonated 4′-aminopyrimidium ion (APH^+), the 1′,4′-iminopyrimidine (IP), and the C_2-ionized ylide (Y), whose formation is believed to activate ThDP to initiate the catalytic cycle in thiamin-dependent enzymes [6–10], **Figure 1**.

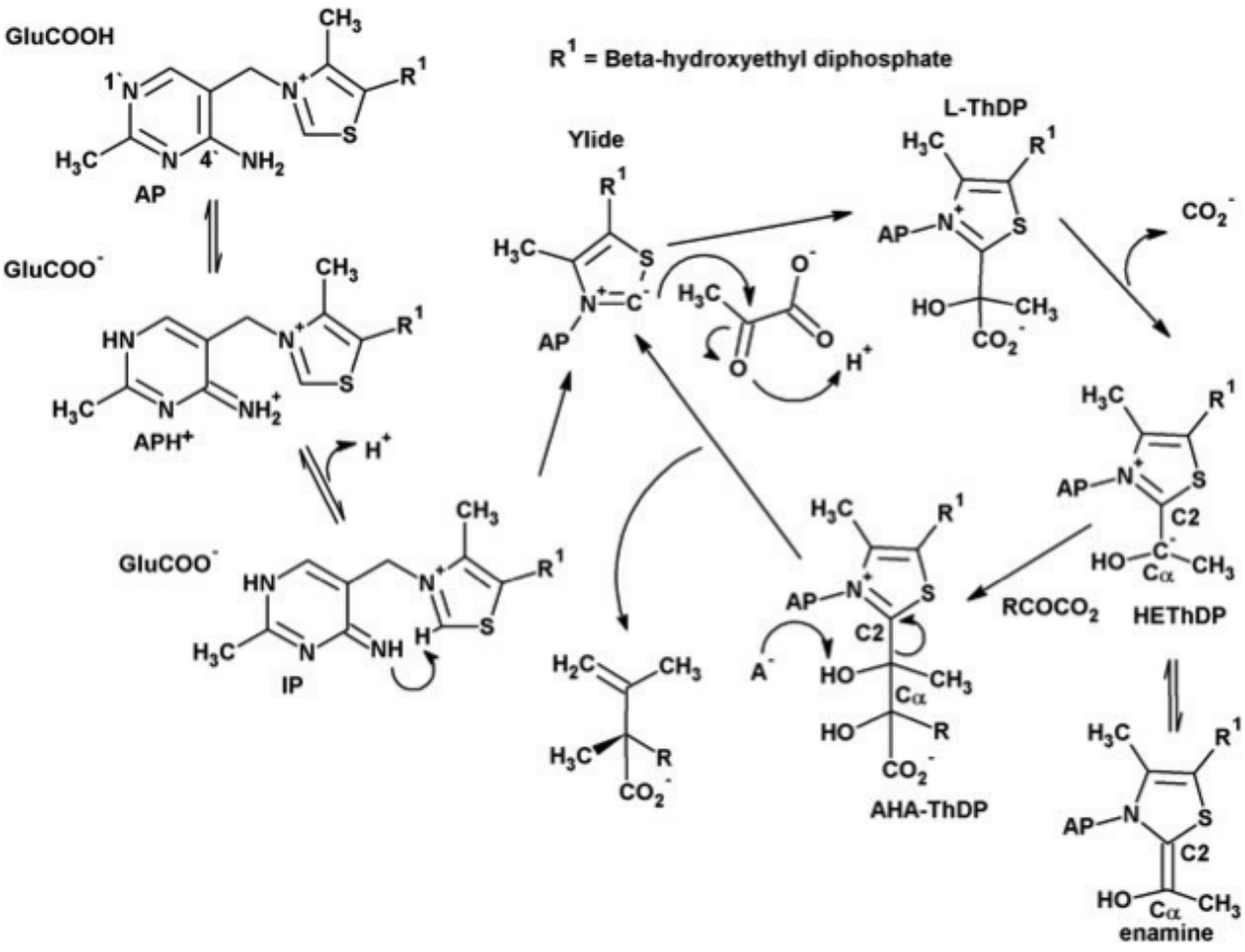

Figure 1. Activation of ThDP and catalytic cycle of AHAS.

In this chapter, we review the results from our group for the different stages of the catalytic cycle of AHAS from a theoretical point of view, using both quantum chemical cluster and Quantum Mechanics/Molecular Mechanics approaches.

2. Activation of thiamin diphosphate (ThDP)

The cofactor ThDP is involved in the sugar metabolism by catalyzing carbon–carbon bond breaking, as well as bond forming [7–9]. During catalysis, the 4′-aminopyrimidine ring can interconvert among four ionization/tautomeric states: AP, APH^+, IP, and the ylide Y (**Figure 2**). In this section, the equilibria among the various ionization and tautomeric states involved in the activation of ThDP and the electron density reactivity indexes of the tautomeric/ionization forms of thiamin diphosphate are addressed using high-level density functional theory calculations.

2.1. Thermodynamics

We have studied the equilibria among the various ionization and tautomeric states involved in the activation of ThDP by using density functional theory calculations at the X3LYP/6-311++G(d,p)//X3LYP(PB)/6-31++G(d,p) level of theory [11, 12]. Briefly, the procedure consists of geometry optimization in solution without any constraint. Solvation effects were modeled using the Poisson-Boltzmann model as implemented in Jaguar. The solvents chosen were water and cyclohexane, as paradigms of polar and apolar media, respectively. All computations were

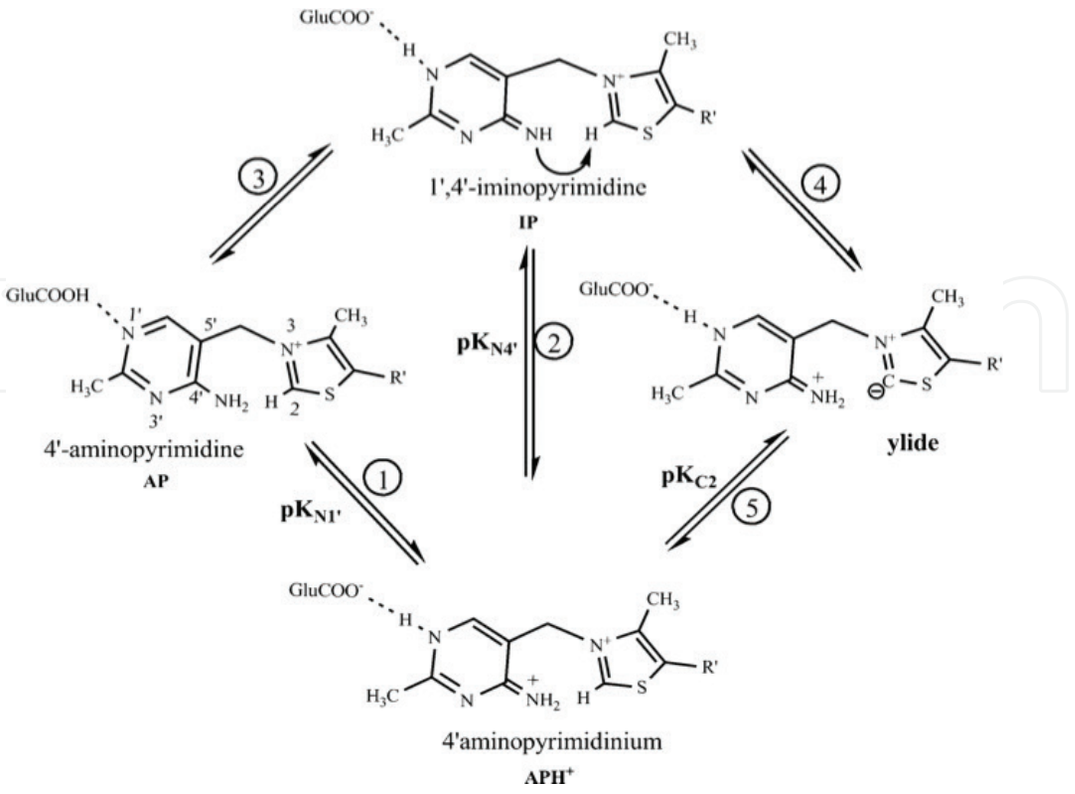

Figure 2. Equilibria among the different tautomeric/ionization forms of thiamin diphosphate.

done considering the highly conserved glutamic residue interacting with the N1′ atom of the 4-aminopyrimidine ring, as a simple way of considering the apoenzymatic environment.

The first equilibrium involves the proton transfer from the glutamic acid side chain to the N1′ atom. In order to evaluate the acidity constant of the N1′ atom, it is necessary to determine the free energy change corresponding to the protonation of the N1′ atom solely. This can be performed applying the Hess's Law considering the following two equations:

$$AP + GluCOOH \leftrightarrow APH^+ + GluCOOH \quad (1)$$

$$GluCOO^- + H^+ \leftrightarrow GluCOOH \quad (2)$$

whose sum gives the desired equation:

$$AP + H^+ \leftrightarrow APH^+ \quad (3)$$

The calculated standard free energy changes for the first equation are −1.1 and +3.0 kcal/mol, in the solvents cyclohexane and water, respectively. While for the second equation, the free energy changes are those that correspond to pKa's values of 4.5 in aqueous solution, and 7 in the enzymatic environment, as predicted by the Propka software. Using these figures, the resulting values of ΔG^0 for Eq. (3) are −3.2 and −10.7 (kcal/mol), in water and cyclohexane, respectively. The results show that the protonation of the N1′ atom is thermodynamically favored in both solvents. The resulting values of pK_{N1}' are 2.32 and 7.81, in water and cyclohexane, respectively. The low value obtained in water is in the characteristic range of a weak acid and do not reflect the well-known basicity of amines. The obtained value in cyclohexane, however, is in the typical range of amines, on the one hand; and it is in agreement with the accepted value of about 7 for glutamates in the proteic ambient, on the other hand.

The second equilibrium involves the transfer of a proton from the N4′ atom to an amino acid side chain, for instance, Glu473 in pyruvate decarboxylase (PDC). Its respective value of the standard free energy change includes the values corresponding to the deprotonation of the N1′ atom and the protonation of glutamate. In order to determine $pK_{N4'}$ we follow an analog procedure to that considered for the first equilibrium. We consider the following chemical equations:

$$APH^+ + GluCOO^- \leftrightarrow IP + GluCOOH \quad (4)$$

$$GluCOOH \leftrightarrow GluCOO^- + H^+ \quad (5)$$

to give the desired equation:

$$APH^+ \leftrightarrow IP + H^+ \quad (6)$$

The resulting values of ΔG^0 for the reaction (6) are +6.0 and +10.6 kcal/mol in water and cyclohexane, respectively. These values imply that this reaction does not proceed spontaneously

under standard conditions. However, at temperature and pressure constant, the spontaneity of a process is given by ΔG and not by ΔG^0. They are related by the well-known relation $\Delta G = \Delta G^0 + RT \ln Q$, where Q is the ratio of the activities of the products to the activities of the reactants. Considering that the concentrations of the different forms of ThDP in the enzyme are quite low, their activity coefficients must not be very different from unity, and consequently, the activities could be replaced by the concentrations. Under this assumption, Q takes the form $[IP][H^+]/[APH^+]$, where the concentration of hydrogen ions is about 10^{-7} mol/L. In consequence under physiological conditions, the reaction becomes thermodynamically favored because of the cancelation of the positive value of ΔG^0 by the contribution of $[H^+]$ to ΔG. The corresponding calculated values of pK_{N4}' are 4.35 and 7.72 in water and cyclohexane, respectively.

The standard free energy change for the third equilibrium, tautomeric equilibrium between AP and IP, can be calculated by combining the chemical Eqs. (3) and (6). The calculated values are +2.8 and -8.3×10^{-2} kcal/mol, for water and cyclohexane, respectively. The corresponding equilibrium constants are 8×10^{-3} and 1.1, respectively. These values imply that in aqueous solution, the formation of IP from AP is thermodynamically forbidden, while the value in cyclohexane is in agreement with the suggested values of about 1 for the equilibrium constant [13].

The fourth equilibrium involves the transformation of IP into the ylide. The calculated values of ΔG^0 are +0.1 and +1.0 kcal/mol, in water and cyclohexane, respectively. The corresponding equilibrium constants are 0.85 and 0.18, respectively. The calculated values are in agreement with the value suggested in the literature of 1–10 for the ratio [IP]/[ylide] [13].

The fifth equilibrium involves the deprotonation of the C_2 atom of APH^+ to form the ylide. The standard free energy change for this reaction can be obtained by combination of the following equations, whose ΔG^0 are known:

$$IP \leftrightarrow ylide \tag{7}$$

$$GluCOOH \leftrightarrow GluCOO^- + H^+ \tag{8}$$

$$APH^+ + GluCOO^- \leftrightarrow IP + GluCOOH \tag{9}$$

Resulting in the desired equation:

$$APH^+ \leftrightarrow ylide + H^+ \tag{10}$$

The calculated values of ΔG^0 are +6.1 and +11.6 kcal/mol, in water and cyclohexane, respectively. These values imply that the ylide is not formed by the direct transformation of APH^+, but via the IP species through via the following sequence: $APH^+ \rightarrow IP \rightarrow$ ylide, as suggested in the literature. On the other hand, the value of ΔG^0 in aqueous solution does not correspond with weakly acidic nature of the thiazolium C_2H group, while its value in cyclohexane is in agreement with the value reported in the literature in the range of 8–9 for the deprotonation of the C_2 atom [13]. **Table 1** summarizes the calculated values of ΔG^0 for the possible equilibria for the diverse tautomeric/ionization forms of ThDP.

Equilibrium	Solvent	Reaction	ΔG^0 (kcal/mol)
1	Cyclohexane	GluCOOH + AP ↔ $GluCOO^-$ + APH^+	−1.1
	Water		+3.0
2	Cyclohexane	APH^+ + $GluCOO^-$ ↔ IP + GluCOOH	+1.0
	Water		−0.2
3	Cyclohexane	AP ↔ IP	−0.083
	Water		+2.8
4	Cyclohexane	IP ↔ ylide	+1.0
	Water		+0.1
5	Cyclohexane	APH^+ ↔ ylide + H^+	+11.6
	Water		+6.1

Table 1. Standard free energy for the possible equilibria of ThDP.

2.2. Electron density reactivity indexes

In order to complement the thermodynamic results described above, the electron density reactivity indexes of the diverse tautomeric/ionization forms of ThDP were calculated using density functional theory (DFT) calculations at the X3LYP/6-31++G(d,p) level of theory. The study includes the calculation of Fukui functions and condensed-to-tom Fukui indices as a means to assess the electrophilic and nucleophilic character of key atoms in the pathway leading to the formation of the ylide [12].

The quantum chemical calculations were performed considering a clusterized model consisting only of ThDP and the conserved chain of glutamic acid interacting with the N1′ atom of the pyrimidyl ring, and the rest of residues were ignored. In order to simplify the calculations, the diphosphate group of ThDP was replaced by a hydroxyl group, having in mind that the primary function of the diphosphate group is to anchor the cofactor, and it is not involved in the catalysis. The geometries of all structures were optimized in gas phase using the same level of theory X3LYP/6-31++G(d,p). All the quantum chemical calculations of the study were performed using Jaguar 7.0 suite of programs.

The generation of the ylide requires the proton abstraction from the C_2 atom by the N4′ atom of the IP form. Therefore, the nucleophilicity of the N4′ atom is essential for the formation of the ylide. Therefore, the Fukui function and the atomic Fukui indices on this atom were calculated for two alternative forms of IP, those having the N1′ atom protonated and deprotonated, respectively. The nucleophilic character of the N4′ atom as expressed by f^-_{N4} f^- Fukui functions is shown in **Figures 3** and **4**. **Figure 3** shows that the isosurface is negligible in the structure having the N1′ atom protonated. On the other hand, **Figure 4** shows that for the N1′ atom deprotonated form, there is an important nucleophilicity on the N4′ atom as required for the proton abstraction from de C_2 atom. In line with the above finding, the respective condensed-to-atom Fukui indices are 0.00 and 0.41, respectively. These results suggest that the imino form should be with the N1′ atom deprotonated in order to favor the proton abstraction. The

http://dx.doi.org/10.5772/intechopen.73705

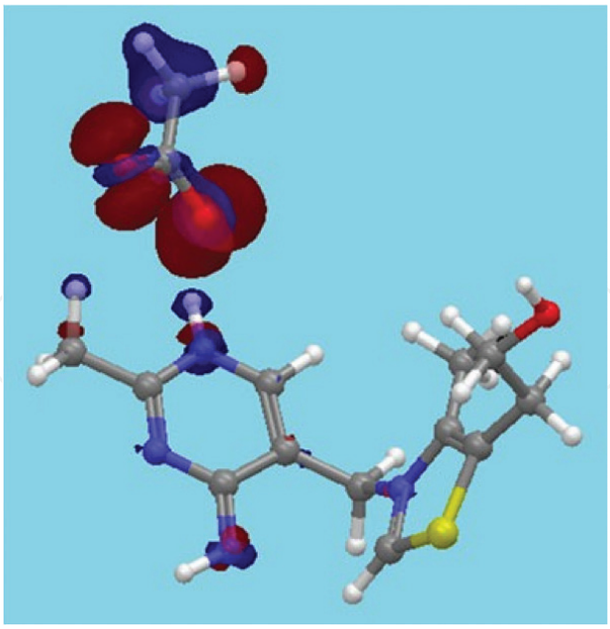

Figure 3. Nucleophilic character of the N1′-protonated IP form as expressed by the *f* − Fukui function.

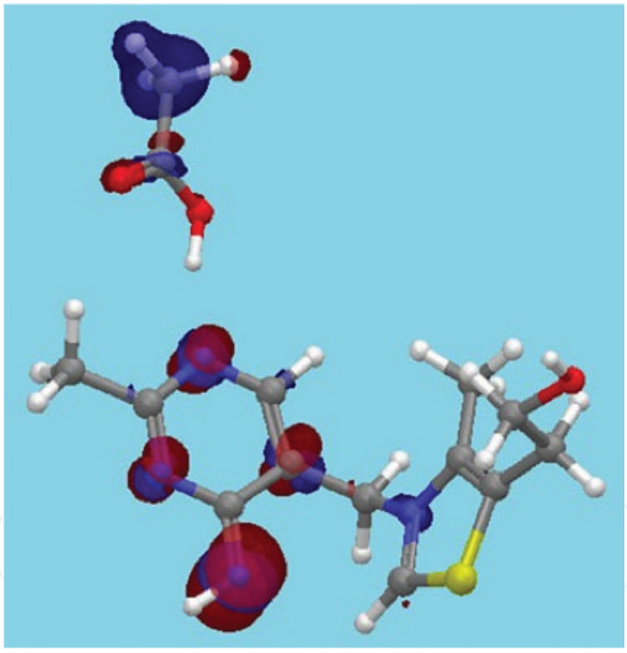

Figure 4. Nucleophilic character of the N1′-deprotonated IP form as expressed by the *f* − Fukui function.

optimization of the structures of both forms of IP shows that the N4′ atom and the proton attached to the C_2 atom are at close distance, 2.39 Å. The transition state associated to this proton transference, **Figure 5**, is characterized with one and only one imaginary frequency, 893.2 cm^{-1}, corresponding to the stretching of the H ↔ C2 bond. The dihedral angles ϕ_t and ϕ_p reach values 67.1^0 and -70.4^0, respectively. In this distorted V–type structure, the N4′atom is only at 1.45 Å from the proton as compared to the rather long C_2-H bond of 1.25 Å. These

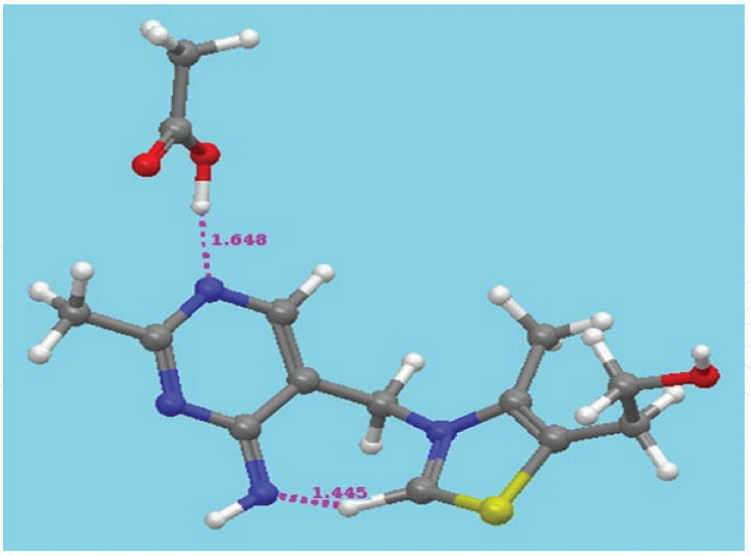

Figure 5. Optimized structure of the transition state for the proton abstraction from the C2 atom.

bond lengths accounts for the proton transfer in progress. The observed activation barrier is just 0.7 kcal/mol, as expected for rapid proton transference. On the other hand, the results show that the reaction of formation of the ylide is exergonic with a standard free energy change of −35.19 kcal/mol.

In ThDP-dependent enzymes, the ylide so formed has the role of to initiate the catalytic cycle with the nucleophilic attack on the C_{α} atom of the pyruvate molecule to form the intermediate lactyl-ThDP. Consequently, the reaction is strongly dependent on the nucleophilic character of the C_2 atom. In order to address this issue, the f^{-}_{C2} Fukui functions were calculated and shown in **Figures 6** and **7**. The results show that only the ylide form having the N1′ atom deprotonated

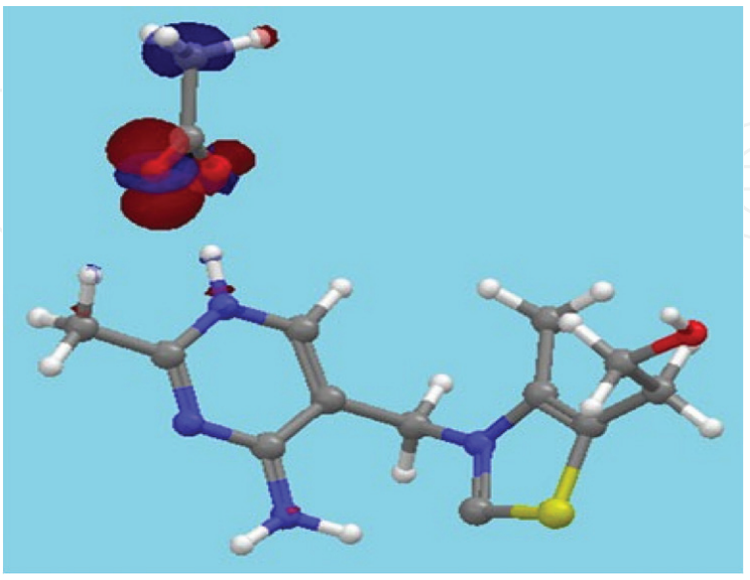

Figure 6. Nucleophilic character of the N1′-protonated ylide form as expressed by the $f-$ Fukui function.

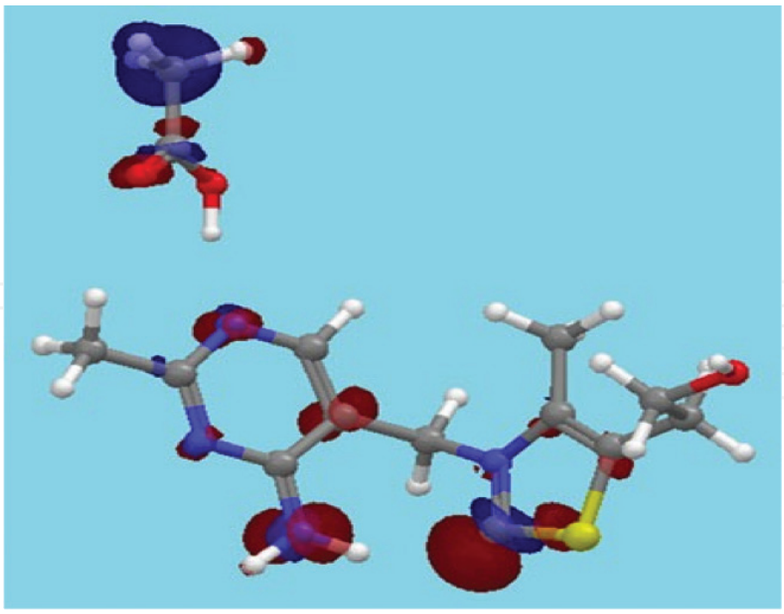

Figure 7. Nucleophilic character of the N1′-deprotonated ylide form as expressed *f* − Fukui function.

shows an important nucleophilicity on the C_2 atom, as required to initiate the catalytic cycle. On the other hand, the other form of the ylide in which the N1′ atom is protonated the C_2 atom does not show any tendency to carry out a nucleophilic attack. Instead, the most important nucleophilic reactivity is lying on the carboxylic oxygen atoms, evidencing the stronger Lewis basicity of these atoms compared to the N1′ atom, and suggesting in turn that the N1′ atom should be deprotonated. The respective atomic Fukui indices on the C_2 atom are 0.00 and 0.34 for the protonated and deprotonated N1′ atom forms, respectively.

2.3. Conclusions

The obtained results in aqueous solution do not correlate with the experimental results; moreover, they cannot be supported from a chemical point of view. Instead, when the enzymatic environment is modeled with a solvent of low dielectric constant, like cyclohexane, the results correlate well both qualitatively and quantitatively to the empirical evidence. In addition, the results show that thermodynamically all ionization/tautomeric forms of ThDP are accessible. The ylide is formed from the IP species as a result of a concerted event in which the increase in the negative partial charge, basicity on the N4′ atom, occurs in conjunction with a decrease in the basicity of the C_2 atom, allowing its deprotonation. The calculated values of pK_a's for the key stages are 7.8, 7.7, and 8.5 for pK_{N1}, pK_{N4}',and pK_{C2}, respectively. These findings support the suggestion given in the literature [14] concerning that the deprotonation and protonation of the C_2 atom are accomplished by a fast proton shuttle enabled by a closely matched pK_a values. The calculated equilibrium constants for the remaining two equilibria are: [IP]/[AP] = 1.2, and [IP]/[ylide] = 5.6. These values are in agreement with those given in the literature [13], of about 1 for equilibrium 3, and values in the range 1–10 for equilibrium 4. In addition, the results allow to conclude that the highly conserved glutamic residue does not protonate the N1′atom of the pyrimidyl ring, but it participates in a strong

hydrogen bonding, stabilizing the eventual negative charge on the nitrogen. This condition provides the necessary reactivity on key atoms, N4′ and C_2, to carry out the formation of the ylide required to initiate the catalytic cycle of ThDP-dependent enzymes.

3. Formation of Lactyl-THDP intermediate

The intermediate Lactyl-ThDP (L-ThDP) is formed in the first stage of the catalytic cycle of AHAS as product of the attack of the ylide on the C_α atom of pyruvate. Despite the number of articles published on the topic, there are still some aspects that remain unknown or controversial, specifically, the manner in which the reaction occurs (i.e., via a stepwise or concerted mechanism) and the protonation states of the N1′ and N4′ atoms during the attack.

In this chapter, we investigate the formation of the L-ThDP intermediate by postulating that the ylide intermediate itself can act as the proton donor, avoiding in this way the involvement of any additional acid-base ionizable group, **Figure 8**. The issue is addressed from a theoretical point of view, considering the total proteic ambient. This chapter includes molecular dynamics simulations, exploration of the potential energy surface (PES) by means of QM/MM calculations, and reactivity analysis on key centers of the reacting species. The PESs are explored for both forms of the ylide, namely, that having the N1′ deprotonated and that having the N1′ atom protonated (henceforth called the Y_1 and Y_2 forms, respectively). The exploration of the PES is carried out in terms of two reaction coordinates accounting for the carboligation and proton transfer. The methodology used has been described earlier in the literature [15].

3.1. Results

The PESs obtained for the two forms of the ylide, Y_1 and Y_2, show very similar topologies, having three critical points that are associated to reactants (R), transition state (TS), and product (P), **Figures 9** and **10**. The topology shows a clear reaction path in which both reaction coordinates vary nearly symmetrically, suggesting a concerted mechanism in which the carboligation and proton transfer occur simultaneously, that is, while the C_2 atom attacks the carbonyl oxygen of pyruvate, the proton of the N4′ amine group is gradually transferred to the carbonyl oxygen of pyruvate as a consequence of the increasing nucleophilic character on the

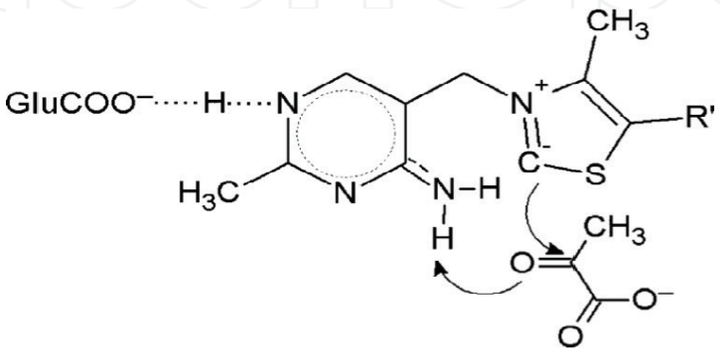

Figure 8. Proposed mechanism for the formation of L-ThDP.

http://dx.doi.org/10.5772/intechopen.73705

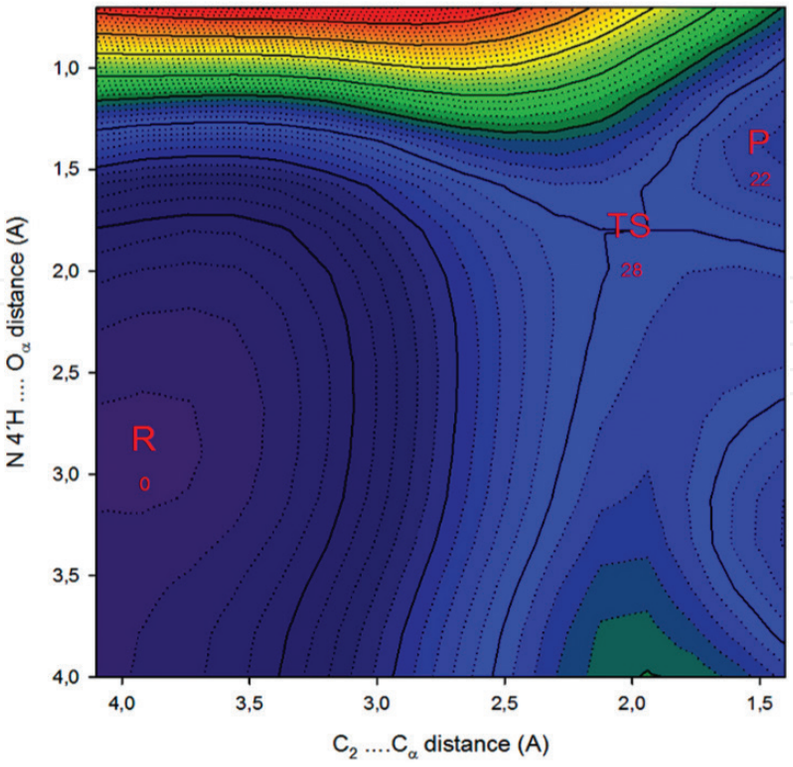

Figure 9. Potential energy surface for the Y_1 form of the ylide.

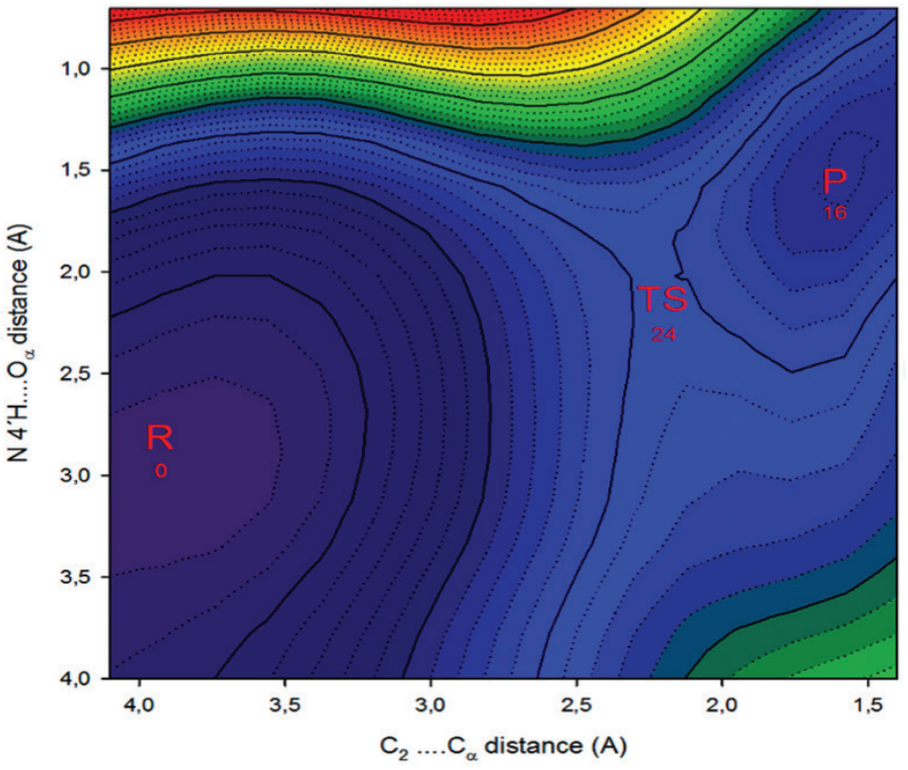

Figure 10. Potential energy surface for the Y_2 form of the ylide.

oxygen atom. On the other hand, the TS of the Y_2 form of the ylide is stabilized in 4 kcal/mol with respect to the TS of the Y_1 form. The respective activation barriers are 28 and 24 kcal/mol. The product, L-ThDP, under the Y_2 form, is stabilized in 6 kcal/mol with respect to the Y_1 form.

The relative stability of the forms Y_1 and Y_2 was assessed by means of the study of the proton transfer from the carboxylic group of Glu139 to the N1′ atom of ThDP. It is found that the Y_2 form (N1′ atom protonated) is energetically lower in about 4 kcal/mol than the Y_1 form. The calculated activation barrier for this proton transference is about 4.5 kcal/mol. These results are summarized in the energy diagram, **Figure 11**. The calculated energy barriers are 28 and 24 kcal/mol for the Y_1 and Y_2 forms, respectively. In consequence, the reaction leading to the formation of L-ThDP should occur under Y_2 form of the ylide. However, the reactivity analysis using the condensed to atom Fukui índices show that at long C_2-C_α distance (reactant state), the nucleophilic character of the C_2 atom is null for the Y_2 form, **Table 2**. On the other hand, an important nucleophilic character on the carboxylic oxygens of Glu139 is observed, strong enough to detach the proton from the N1′ atom located at close distance, about 1.8 Å. These findings suggest that reaction cannot be initiated under the Y_2 form. Unlike, the Y_1 form shows non-null nucleophilic character on the C_2 atom at early stages of the reaction suggesting that the reaction should be initiated under this form.

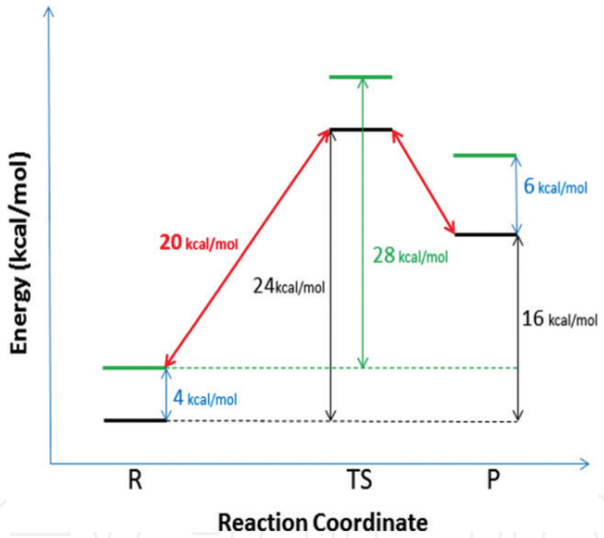

Figure 11. Schematic energy profile for the reaction (red: minimum-energy path; green: Y_1 form of the ylide; black: Y_2 form of the ylide).

	Y_1			Y_2	
C_2–C_α distance (Å)	C_2	O_α	$GluCOO^-$	C_2	O_α
4.0	0.02	0.00	0.50	0.00	0.00
3.5	0.29	0.02	0.50	0.00	0.00
3.0	0.57	0.04	0.00	0.51	0.07
2.5	0.49	0.11	0.00	0.50	0.12

Table 2. Nucleophilic character on selected atoms as expressed by the f^- Fukui index.

Having in mind the energetics and reactivity results, it is possible to postulate the following reaction path of minimum energy: the reaction is initiated with the attack of the ylide, in its Y_1 form, on the carbonylic carbon of pyruvate to reach a transition state in which the N1′ atom is protonated. This postulated mechanism allows to reduce the activation barrier to 20 kcal/mol, in agreement with the experimental evidence [15].

4. Formation of 2-aceto-2-hydroxybutyrate

The second stage of the catalytic cycle of AHAS involves the decarboxylation of the L-ThDP intermediate to form the 2-hydroxyethyl-ThDP carbanion/enamine ($HEThDP^-$) intermediate. Then, HEThDP reacts with 2-ketobutyrate (2 KB) to form the 2-aceto-2-hydroxybutyrate (AHA-ThDP) intermediate. In this chapter, the formation of the 2-aceto-2-hydroxybutyrate (AHA-ThDP) intermediate is addressed from a theoretical point of view by means of hybrid quantum/molecular (QM/MM) mechanical calculations [18]. The QM region includes one molecule of 2-KB, the $HEThDP^-$ intermediate, and the residues Arg380 and Glu139, whereas the MM region includes the rest of the protein. This chapter includes potential energy surface (PES) scans to identify and characterize critical points on it, transition state search and activation energy calculations.

The initial structure of AHAS-HEThDP-2 KB for the exploration of the PES was obtained from the solvated and equilibrated structure of AHAS in complex with pyruvate and HEThDP after 15 ns molecular dynamics (MD) simulation, according to the methodology elsewhere [18–20]. Along the simulation, significant displacements of the residues were not observed. In consequence, to model the reaction mechanism, we took the final MD structure as a single representative configuration. This structure was trimmed to a sphere of radius of 30 Å with center at the C_α atom of the $HEThDP^-$ intermediate. Then, the 2 KB structure was superimposed on the structure of pyruvate, and this was deleted.

The reaction mechanism was described on a single PES as a function of two asymmetric reactions coordinates. The reaction coordinate R_1 is defined as the bond length difference between C_α–C_2 and C_α–C_B bonds; the reaction coordinate R_2 is defined as the bond length difference between O_α–H_α and O_B–H_α.

4.1. Results

The PES obtained shows five critical points that are associated to reactants (R), transition states (TS_1 and TS_2), intermediate (I), and product (P), **Figures 12** and **13**. The PESs suggest that the reaction is initiated with the nucleophilic attack of the carbanion on the carbonylic carbon of 2 KB, reaching a transition state TS_1 located at $R_1 \sim -1.0$ and $R_2 \sim -0.6$, evidencing that the nucleophilic attack is in progress while the hydroxyl proton of $HEThDP^-$ remains at constant distance of about 1.7 Å., from the carbonyl oxygen of ketobutyrate, **Figure 14**.

Once the transition state is reached, the PES shows a concerted asynchronous mechanism, namely, the nucleophilic attack continues until R_1 reaches the values of about −0.3; afterward, the proton transfer from the hydroxyl of $HEThDP^-$ to the carbonyl oxygen of ketobutyrate

occurs, leading to the intermediate located at R_1 ~ −0.25 and R_2 ~ 0.75, indicating that at this point the proton transfer has been completed, **Figure 15**.

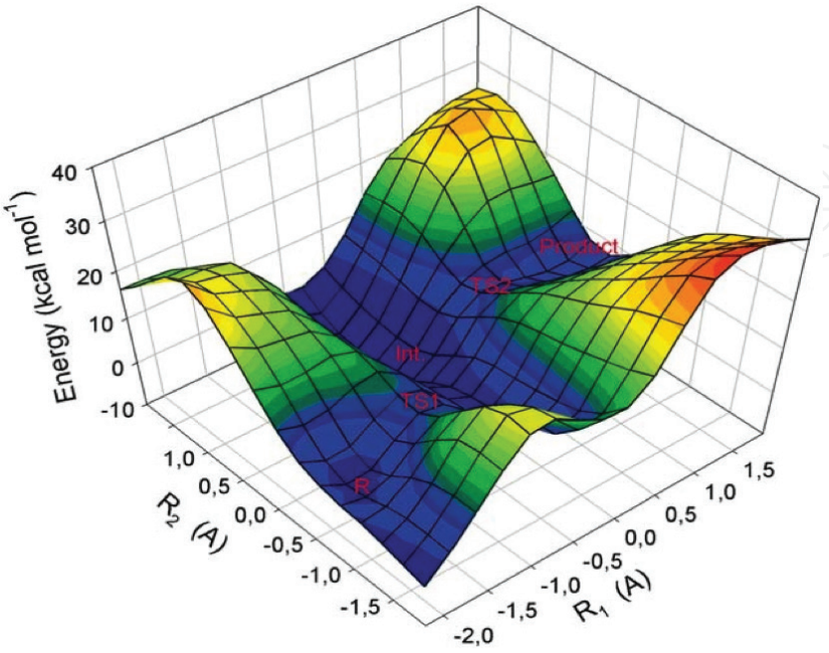

Figure 12. 3-D view of the DFT corrected PES.

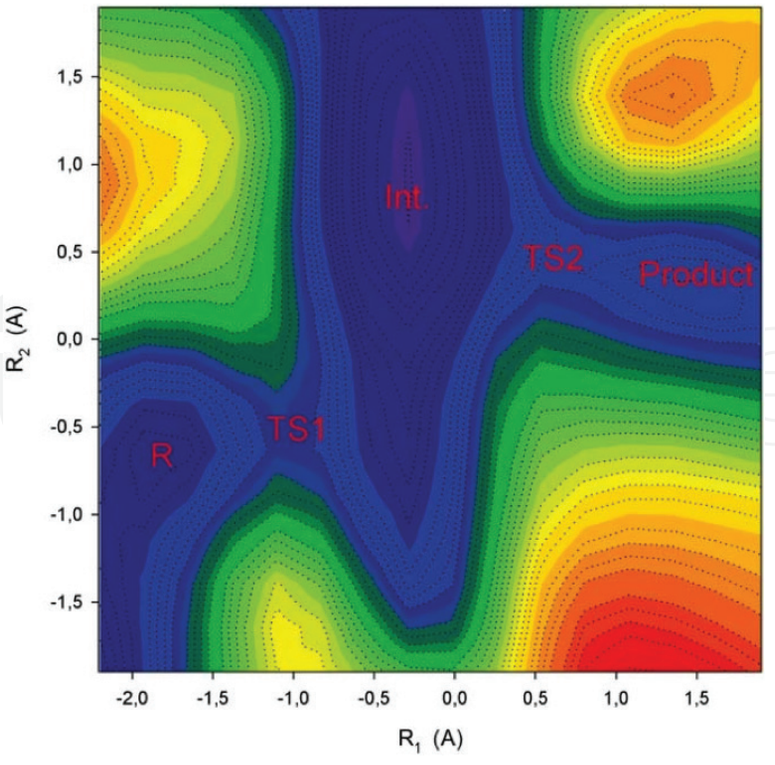

Figure 13. 2-D view of the DFT corrected PES.

http://dx.doi.org/10.5772/intechopen.73705

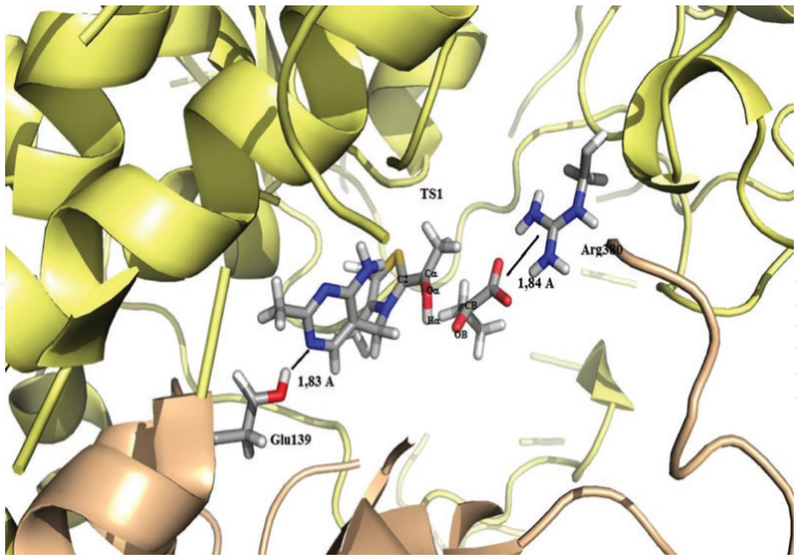

Figure 14. Optimized geometry of the transition state TS1.

The reaction continues with the increase of the reaction coordinate R_1 reaching the second transition state TS2 located at coordinates R_1 ~ 0.5 and R_2 ~ 0.5, **Figure 16**. The reaction path for this event is clearly observed on the PES; in this step, the reaction proceeds at R_2 constant, while the coordinate R_1 changes systematically toward positive values indicating the separation of the product from the C_2 atom of the thiazolium ring of ThDP, and the consequent ylide regeneration is in progress, **Figure 17**. The relevant distances and relative energies of the critical points observed in the PES are summarized in **Table 3**. It is observed the gradual shortening of the distance C_α–C_B and lengthening of the distance C_α–C_2 when going from reactant to product, accounting for the nucleophilic attack and product release. Similar trend for the distances

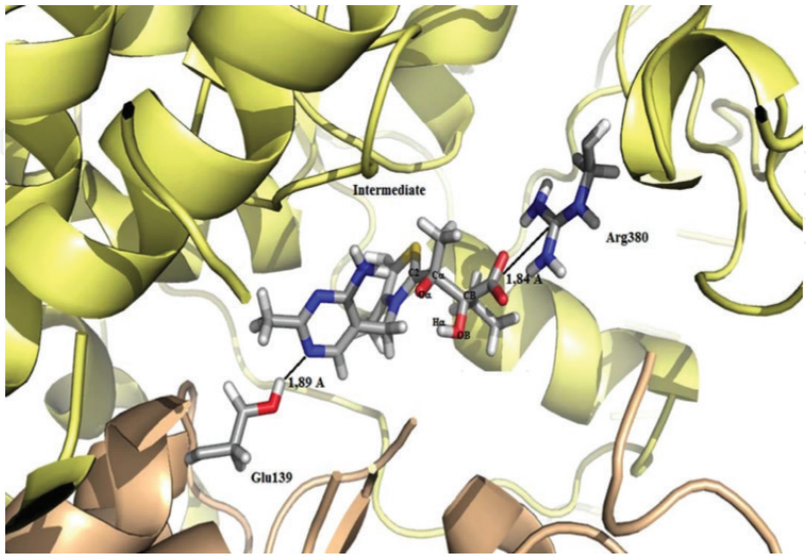

Figure 15. Optimized geometry of the intermediate.

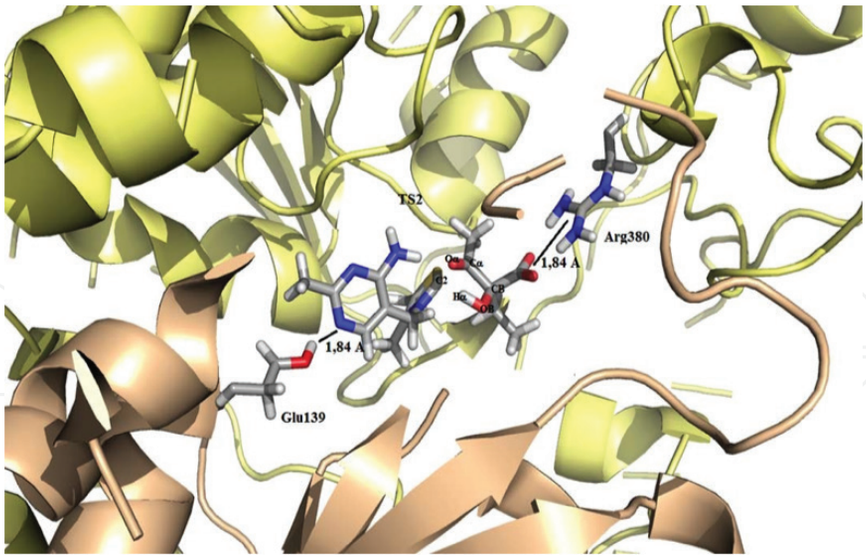

Figure 16. Optimized geometry of the transition state TS2.

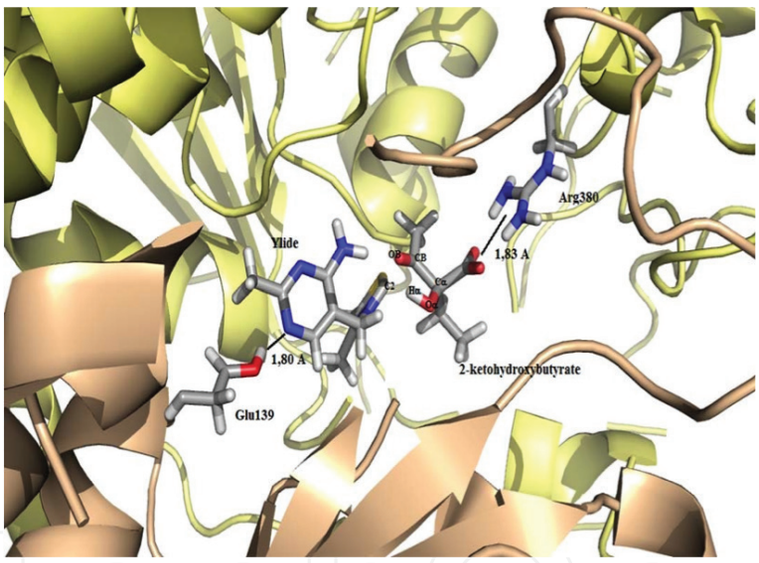

Figure 17. Optimized geometry of the product.

	Reactant	TS1	Intermediate	TS2	Product
C_{α}–C_2 (Å)	1.37	1.43	1.51	2.30	3.48
C_{α}–C_B (Å)	3.28	2.35	1.80	1.60	1.56
O_{α}–H_{α} (Å)	1.02	0.98	1.94	1.60	1.71
O_B–H_{α} (Å)	1.55	1.69	0.95	1.02	1.00
Relative energy (kcal/mol)	0.0	11.0	−9.0	6.10	3.00

Table 3. Interatomic distances and relative energies of the critical points on the PES.

O_{α}–H_{α} and O_{B}–H_{α} is observed as long as the reaction proceeds. The respective activation barriers are 11 and 15 kcal/mol, evidencing that the second stage is the rate controlling step, in agreement with the empirical evidence.

4.2. Conclusions

The main conclusions can be summarized as follows: (1) the reaction between the intermediate HEThDP^{-} and 2-ketobutyrate occurs via a stepwise mechanism consisting of two steps; (2) the first reaction step corresponds to the nucleophilic attack of the carbanion on the carbonylic carbon of 2-KB; this stage occurs via a concerted asynchronous mechanism, that is, the proton transfer follows the carboligation event; (3) the second reaction stage involves the product release and ylide recovery, allowing in this way to reinitiate the catalytic cycle once more; (4) two transition states are observed on the PES, the first one, TS1 corresponding to the first reaction step, has an activation barrier of about 11 kcal/mol, while the second one, TS2 corresponding to the product liberation, has an activation barrier of about 15 kcal/mol. (5) The results are in agreement with literature values [16, 17] which states that the next step to the formation of the adduct is the rate controlling step among the last two stages of the AHAS catalytic cycle.

Acknowledgements

The author acknowledges financial support from FONDECYT grants 1130082 and 1170091.

Author details

Eduardo J. Delgado

Address all correspondence to: edelgado@udec.cl

Computational Chemistry Group, Faculty of Chemical Sciences, Universidad de Concepción, Concepción, Chile

References

[1] Duggleby RG, Pang SS. Acetohydroxyacid synthase. Journal of Biochemistry and Molecular Biology. 2000;**33**:1-36

[2] Pang S, Duggleby RG, Guddat LW. Crystal structure of yeast acrtohydroxyacid synthase: A target for herbicidal inhibitors. Journal of Molecular Biology. 2002;**317**:249-262

[3] Chipman DM, Duggleby RG, Tittmann K. Mechanisms of acetohydroxyacid synthases. Current Opinion in Chemical Biology. 2005;**9**:475-481

[4] McCourt JA, Duggleby RG. Acetohydroxyacid synthase and its role in the biosynthetic pathway for branched-chain amino acids. Amino Acids. 2006;**31**:173-210

[5] Gedi V, Yoon MY. Bacterial acetohydroxyacid synthase and its inhibitors – A summary of their structure, biological activity and current status. The FEBS Journal. 2012;**279**:946-963

[6] Kluger R, Tittmann K. Thiamin diphosphate catalysis: Enzymatic and nonenzymic covalent intermediates. Chemical Reviews. 2008;**108**:1797-1833

[7] Jordan F, Nemeria NS. Experimental observation of thiamin diphosphate-bound intermediates on enzymes and mechanistic information derived from these observations. Bioorganic Chemistry. 2005;**33**:190-215

[8] Agyei-Owusu K, Leeper FJ. Thiamin diphosphate in biological chemistry: Analogues of thiamin diphosphate in studies of enzymes and riboswitches. The FEBS Journal. 2009;**276**:2906-2916

[9] Kern D, Kern G, Neef Holger TK, Killenberg-Jabs M, Wikner C, Schneider G, Hübner G. How thiamine diphosphate is activated in enzymes. Science. 1997;**275**:67-70

[10] Nemeria NS, Chakraborty S, Balakrishnan A, Jordan F. Reaction mechanisms of thiamin diphosphate enzymes: Defining states of ionization and tautomerization of the cofactor at individual steps. The FEBS Journal. 2009;**276**:2432-2446

[11] Delgado EJ, Alderete JB, Jaña GA. Density-functional study on the equilibria in in the ThDP activation. Journal of Molecular Modeling. 2011;**17**:2735-2739

[12] Jaña GA, Delgado EJ. Electron density reactivity indexes of the tautomeric/ionization forms of thiamin diphosphate. Journal of Molecular Modeling. 2013;**19**:3799-3803

[13] Nemeria N, Korotchkina L, McLeish MJ, Kenyon GL, Patel MS, Jordan F. Elucidation of the chemistry of enzyme-bound thiamin diphosphate prior to substrate binding: Defining internal equilibria among tautomeric and ionization states. Biochemistry US. 2007;**46**:10739-10744

[14] Tittmann K, Neef H, Golbik R, Hubner G, Kern D. Kinetic control of thiamin diphosphate activation in enzymes studied by proton-nitrogen correlated NMR spectroscopy. Biochemistry US. 2005;**44**:8697-8700

[15] Lizana I, Delgado EJ. New insights on the reaction pathway leading to lactyl-ThDP: A theoretical approach. Journal of Chemical Information and Modeling. 2015;**55**:1640-1644

[16] Friedemann R, Titmann K, Golbik R, Hübner G. DFT and MP2 stdies on the C_2–$C_{2\alpha}$ bond cleavage in thiamin catalysis. Journal of Molecular Catalysis B: Enzymatic. 2009;**61**:36-38

[17] Alvarado O, Jaña G, Delgado EJ. Computer-assisted study on the reaction between pyruvate and ylide in the pathway leading to lactyl-ThDP. Journal of Computer-Aided Molecular Design. 2012;**26**:977-982

[18] Sanchez L, Jaña GA, Delgado EJ. A QM/MM study on the reaction pathway leading to 2-aceto-2-hydroxybutyrate in the catalytic cycle of AHAS. Journal of Computational Chemistry. 2014;**35**:488-494

[19] Jaña G, Jimenez V, Villa-Freixa J, Prat-Resina X, Delgado E, Alderete J. Computational study on the carboligation reaction of acetohydroxyacid synthase: New approach on the role of the HEThDP intermediate. Proteins. 2010;**78**:1774-1788

[20] Jaña G, Jimenez V, Villa-Freixa J, Prat- Resina X, Delgado E, Alderete JB. A QM/MM study on the last two steps of the catalytic cycle of acetohydroxyacid synthase. Computational & Theoretical Chemistry. 2011;**966**:159-166

IntechOpen

IntechOpen